

## Optical analysis of the Pacific Ocean Neutrino Experiment (P-ONE) site using data from the first pathfinder mooring

**Christian Fruck,<sup>a,\*</sup> Andreas Gärtner,<sup>b</sup> Immacolata Carmen Rea<sup>a</sup> and Jakub Stacho<sup>c</sup>**  
**on behalf of the P-ONE Collaboration**

(a complete list of authors can be found at the end of the proceedings)

<sup>a</sup>*Technical University Munich, Physics Department,  
James-Frank-Str. 1, Garching bei München, Germany*

<sup>b</sup>*University of Alberta, Department of Physics,  
Edmonton, Alberta, Canada*

<sup>c</sup>*Simon Fraser University, Department of Physics,  
Burnaby, British Columbia, Canada*

*E-mail: [cfruck@ph.tum.de](mailto:cfruck@ph.tum.de), [gaertner@ualberta.ca](mailto:gaertner@ualberta.ca), [imma.rea@tum.de](mailto:imma.rea@tum.de),  
[jakubs@sfu.ca](mailto:jakubs@sfu.ca)*

The Pacific Ocean Neutrino Experiment (P-ONE) is an initiative by a collaboration of Canadian and German universities as well as Ocean Networks Canada (ONC) to develop a new large-scale neutrino telescope 2600 m below the ocean off the coast of western Canada. While the instrumented volume needs to be at least on the order of km<sup>3</sup> for the physics goals of P-ONE to be met, the density of photo sensors needs to be kept as low as possible in order to minimize construction costs. Naturally, this puts very high demands on the optical properties of water at the deployment site. Ideally, the water should exhibit minimal photon extinction and scattering to optimize the light yield and timing needed for reconstructing neutrino-induced Cherenkov light flashes. In addition, a low light background from natural undersea sources such as bioluminescence and K40 radioactive decay is necessary for achieving high sensitivity to neutrino events. In order to evaluate the proposed site for P-ONE, two pathfinder missions have been deployed successfully, one in 2018 and the other in 2020. We present the results from the first mission that was primarily aimed at evaluating the optical properties of the site in terms of attenuation length, and backgrounds.

*37<sup>th</sup> International Cosmic Ray Conference (ICRC 2021)  
July 12th – 23rd, 2021  
Online – Berlin, Germany*

---

\*Presenter

## 1. Introduction

The Pacific Ocean Neutrino Experiment (P-ONE) is a new project[1], backed by a growing collaboration of scientists from Germany, Canada, and the USA, with the goal of constructing a  $\text{km}^3$ -scale neutrino telescope in the Cascadia Basin region of the Pacific Ocean, off the coast of British Columbia, Canada. P-ONE is supported by the Canadian oceanographic institute Ocean Networks Canada (ONC). The Cascadia Basin site where P-ONE is intended to be deployed is part of ONC's NEPTUNE observatory, an 800 km electro-optical fiber loop with several access nodes hosting numerous scientific instruments.

As a pathfinder mission for the P-ONE detector, a pair of mooring lines named STRings for Absorption length in Water (STRAW) was been deployed in 2018. The goal of STRAW was to measure the optical properties of the Cascadia Basin water as well as the in-situ ambient light levels [2]. The experiment consists of two 150 m long mooring lines a distance of 37 m from one another. Optical modules are mounted along each mooring line at heights of 30 m, 50 m, 70 m, and 110 m above the seabed. Of these modules, three are POCAMs (Precision Optical CALibration Modules, originally developed as isotropic light emitters for an upgrade of the IceCube detector [3]). These act as light emitters, while the remaining five modules are optical receivers called sDOMs (STRAW Digital Optical Modules), consisting of two photomultiplier tubes (PMTs) with a time-over-threshold (ToT) readout system inside a pressure-resisting housing.

STRAW was deployed in June 2018 and then commissioned through the rest of the year. Since commissioning, STRAW has been operating live with an average 98% live time. There are two main measurements that STRAW is designed to make. The first is to determine the optical attenuation length of the water at the P-ONE candidate site. This measurement is performed by emitting short (7 ns) pulses with LEDs of four different wavelengths: 365 nm, 400 nm, 450 nm, and 585 nm. These flashes are received by the sDOMs and can be distinguished from background via the flasher periodicity. Measurements are made with a number of sDOM-POCAM configurations and performed about once per month. For this measurement, the DAQ of the sDOMs record the timestamp of all arriving photons with sub-ns precision, generating  $\sim 200$  MB per minute per sDOM. Therefore the experiment can only be operated for  $\sim 1$  min per POCAM and LED intensity in this configuration.

The other operating mode complements the second goal of STRAW, measuring the ambient light background at the Cascadia Basin site which is primarily caused by undersea bioluminescence and radioactivity. This measurement does not require perfect timing for single photon events. Rather, it can be performed by only measuring the rates of single photo-electron events at the PMTs. Therefore, counters that register these events, even if no time stamps are recorded, are sampled 30 times per second over the entire live time of the instrument which is now well over two years.

This paper describes the analysis method for extracting the attenuation length from the POCAM flasher data and the results from this study. Additionally the results from the ambient light study are presented.

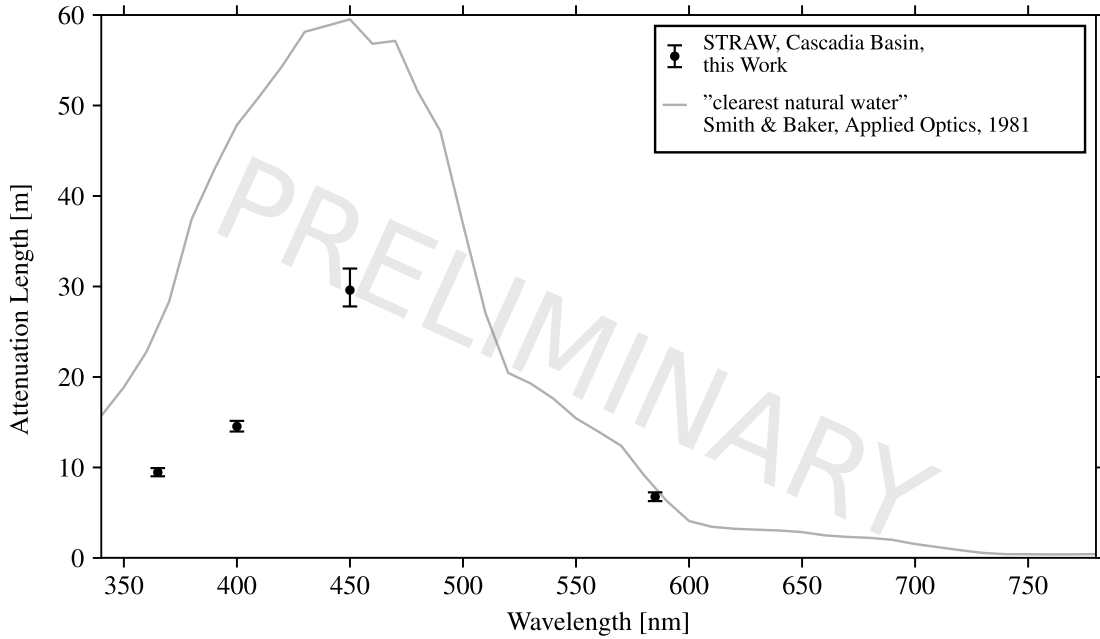


**Figure 1:** Attenuation length vs. wavelength from the simultaneous multi-wavelength fit of all available STRAW data compared to a study of attenuation lengths in the clearest ocean waters [4].

## 2. Attenuation Length Measurements

The optical properties of the water at the P-ONE site are critical for the success of the experiment. One of the fundamental quantities that strongly influence the design of P-ONE is the attenuation length, this property sets the scale for how far the optical modules will be set on the mooring lines as well as the distance between the lines. The attenuation measurement is performed using the POCAM flashers and locking into the pulse frequency signal in the sDOM data.

The DAQ system of the sDOM records timestamps of the pulse trigger times and time-over-threshold (TOT), this level of information is not well suited for resolving multiple photon pulses. The flasher intensities used for the attenuation length analysis are adjusted such that the average number of photons recorded in an sDOM PMT is  $< 1$ . From Poisson statistics it can be derived that for an average intensity in terms of photons hitting and being detected by the photo sensor, per flash  $\overline{N}_{\text{ph}}$ , the average fraction of flashes that cause the detector to record a photon hit fraction  $h$  can be expressed as follows.

$$h = 1 - P_{\overline{N}_{\text{ph}}}(0) = e^{-\overline{N}_{\text{ph}}}. \quad (1)$$

This number is an easily accessible and reliably measurable observable for the STRAW setup and has therefore been used for deriving the attenuation length.

For the analysis of STRAW data, a Bayesian approach has been chosen because it facilitates the consideration of systematic uncertainties as nuisance parameters. Using this approach, the uncertainty is expressed as a parameter prior. Another advantage of the Bayesian approach is that it allows combination of many measurements, even those recorded using different LEDs by

constructing a joint likelihood function. The following model is used for predicting the hitfraction from a specific combination and configuration of POCAM and sDOM:

$$\overline{N_{\text{ph}}} = P \cdot S \cdot N_0(U) \cdot \frac{R^2 \pi}{4\pi d^2} \cdot e^{-\frac{d}{\lambda}} \cdot \epsilon \cdot Q \cdot \Pi(\theta) \cdot \Sigma(\theta), \quad (2)$$

where  $P$  is a correction factor for the light yield emitted by the POCAM and  $S$  is a correction factor for the detection efficiency of the sDOM.  $N_0(U)$  is the number of photons emitted into  $4\pi$  sr, extrapolated from a lab calibration that measured the amount of light emitted in the forward direction. The quotient with  $d^2$  in the denominator describes the geometrical dilution of light, characterized by the distance between sDOM and POCAM  $d$  and the radius of the photocathode of the PMT  $R$ .  $\lambda$  is the attenuation length and therefore the actually sought after parameter when fitting the model.  $\epsilon$  and  $Q$  are the trigger efficiency for single photons and the PMT quantum efficiency, respectively.

$$\Sigma(\theta) = \left| \cos\left(\frac{\theta}{2}\right)^\gamma \right|, \quad (3)$$

is the angular acceptance profile of an sDOM that has been characterized in a lab measurement, where  $\theta$  is the angle between the symmetry axis of the sDOM and the direction to the light source and  $\gamma$  is a shape parameter that if increased makes the acceptance profile more selective for the forward direction.

$$\Pi(\theta) = 0.75 + 0.25 \cdot |\cos(\theta)^{\frac{2}{3}}| \quad (4)$$

is the angular light emission profile of the POCAM, which has been measured in the lab prior to deployment. The model also includes an additional parameter  $y_{\text{off}}$  that introduces a vertical offset between the two moorings, or a tilt of the moorings in the current; these are indistinguishable in STRAW measurements. The hitfraction can then be calculated according to Equation 1.

The likelihood formulation that is used for the fit assumes simple Gauss-shaped measurement uncertainties:

$$\log(\mathcal{L}) = \sum_{i=1}^N -\frac{(h_i - h_{i,\text{model}})^2}{\Delta h_i^2}. \quad (5)$$

Here  $i$  runs over  $N$  individual hitfraction measurements  $h_i$  with uncertainties  $\Delta h_i^2$ .

A Gaussian prior is used for all nuisance parameters, as listed in table 1. The comparably large uncertainties that are assumed for the individual sDOM trigger efficiencies and also an additional global trigger threshold efficiency serve as a conservative incorporation of eventual systematic uncertainties in the calibration of the sDOMs. These devices have only been calibrated under lab conditions at around 20 degC. An in-situ verification of the trigger sensitivity is not possible. Due to the large number of different combinations of emitters and detectors, as well as even different LEDs and flasher intensities, these substantial uncertainties are marginalized and only result in a moderate increase of the uncertainty in the attenuation length.

The posterior probability distribution is obtained applying a Markov-Chain Monte Carlo (MCMC) approach using the Python package *emcee* [5]. As previously mentioned, several measurements with different combinations of sDOMs and POCAMs, flasher intensities, and different wavelengths, are combined by summing the log-likelihood values.

**Table 1:** Full list of parameters for the joint likelihood formulation. Parameter priors in terms of Gaussian mean and standard deviation are given where applicable. The comparably large uncertainties that are assumed for the individual sDOM trigger efficiencies and also an additional global trigger threshold efficiency serve as a conservative incorporation of eventual systematic uncertainties in the calibration of the sDOMs.

| Parameter                | Description                  | Prior                             |
|--------------------------|------------------------------|-----------------------------------|
| $\lambda_{365\text{nm}}$ | attenuation length           | none                              |
| $\lambda_{400\text{nm}}$ | attenuation length           | none                              |
| $\lambda_{450\text{nm}}$ | attenuation length           | none                              |
| $\lambda_{585\text{nm}}$ | attenuation length           | none                              |
| $Q_{365\text{nm}}$       | PMT quantum efficiency       | $0.24 \pm 0.02$                   |
| $Q_{400\text{nm}}$       | PMT quantum efficiency       | $0.24 \pm 0.02$                   |
| $Q_{450\text{nm}}$       | PMT quantum efficiency       | $0.21 \pm 0.02$                   |
| $Q_{585\text{nm}}$       | PMT quantum efficiency       | $0.04 \pm 0.01$                   |
| $\epsilon$               | trigger threshold efficiency | $0.75 \pm 0.25$                   |
| $\gamma$                 | cosine power sDOM            | $4.0 \pm 0.2$                     |
| $y_{\text{off}}$         | vertical offset              | $0.0 \text{ m} \pm 1.0 \text{ m}$ |
| $P_{1,365\text{nm}}$     | POCAM 1 light yield corr.    | $1.0 \pm 0.1$                     |
| $P_{2,365\text{nm}}$     | POCAM 2 light yield corr.    | $1.0 \pm 0.1$                     |
| $P_{1,400\text{nm}}$     | POCAM 1 light yield corr.    | $1.0 \pm 0.1$                     |
| $P_{2,400\text{nm}}$     | POCAM 2 light yield corr.    | $1.0 \pm 0.1$                     |
| $P_{1,450\text{nm}}$     | POCAM 1 light yield corr.    | $1.0 \pm 0.1$                     |
| $P_{2,450\text{nm}}$     | POCAM 2 light yield corr.    | $1.0 \pm 0.1$                     |
| $P_{1,585\text{nm}}$     | POCAM 1 light yield corr.    | $1.0 \pm 0.1$                     |
| $P_{2,585\text{nm}}$     | POCAM 2 light yield corr.    | $1.0 \pm 0.1$                     |
| $S_1$                    | sDOM 1 det. efficiency corr. | $1.0 \pm 0.25$                    |
| $S_2$                    | sDOM 2 det. efficiency corr. | $1.0 \pm 0.25$                    |
| $S_3$                    | sDOM 3 det. efficiency corr. | $1.0 \pm 0.25$                    |
| $S_4$                    | sDOM 4 det. efficiency corr. | $1.0 \pm 0.25$                    |
| $S_5$                    | sDOM 5 det. efficiency corr. | $1.0 \pm 0.25$                    |

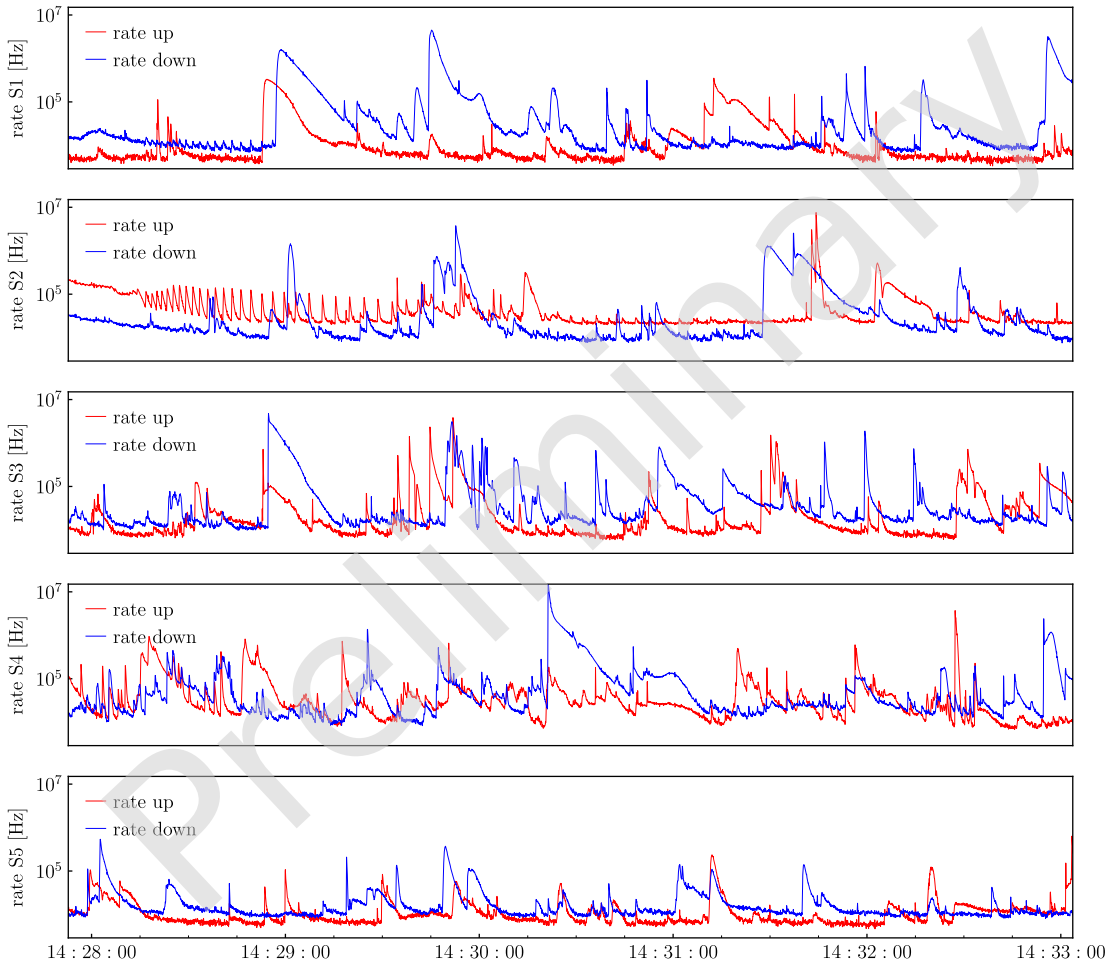
The preliminary results of this study in terms of attenuation length are shown in Table 2 and also illustrated and compared to attenuation lengths in the clearest known ocean waters according to [4] in Figure 1.

### 3. Background Study

While the high precision data during POCAM and sDOM activity is collected for only a small fraction of the live time of STRAW, the the pulse rate counters have been continuously logged over the entire live time at a readout frequency of 30 Hz. Figure 2 shows a five minute example of rates measured in all PMTs. The full data set shows a constant baseline on the order of 10 kHz, while another variable component regularly reaches rates on the order of MHz (< 90% of the time), but

**Table 2:** Results of the combined attenuation-length model fit , using all available data (Preliminary).

| Effective Central Wavelength | Attenuation length     |
|------------------------------|------------------------|
| 365 nm                       | $9.5^{+0.5}_{-0.4}$ m  |
| 400 nm                       | $14.5^{+0.6}_{-0.6}$ m |
| 450 nm                       | $29.6^{+2.4}_{-1.8}$ m |
| 585 nm                       | $6.8^{+0.5}_{-0.5}$ m  |

**Figure 2:** Five minute example of rates measured in all STRAW sDOMs, in both PMTs (looking up and looking down) each. STRAW has been recording data with this resolution, nearly uninterruptedly since early 2018.

can even go as high as the DAQs saturation limit of around 10 MHz. Such high rates are only recorded during a  $\sim 0.5\%$  fraction of the live time.

The baseline background is primarily due to the Cherenkov emission of charged particles

originating in the decay of radioactive elements dissolved in the seawater. In particular, high-energy electrons produced by the beta decay of the  $^{40}\text{K}$  potassium isotope are the most abundant contributors to the radioactive background. Thoroughly understanding and characterizing this radioactive background studied by STRAW plays a significant roll in future neutrino telescope trigger development.

The second, more stochastic contribution to the background comes from marine bioluminescence. Bioluminescence consists of the light emission by a living organism, as a consequence of a chemical process triggered by mechanic, electric, or light stimuli. In particular, light can be emitted after organisms collide with submerged structures. Additionally, bioluminescence can be influenced by environmental parameters such as tides, temperature, and oxygen concentration in the water.

With its diffuse component, bioluminescence can also contribute to the baseline background. For this reason, a full and detailed characterization of this phenomenon represents an essential milestone for the feasibility study of an underwater neutrino detector. One of the principal scientific goals of the STRAW pathfinder was the long term monitoring of bioluminescence activities in the Cascadia Basin site.

#### 4. Summary

The STRAW pathfinder was deployed as a precursor to the P-ONE neutrino telescope to study the in situ optical properties and backgrounds in the Cascadia Basin. After over two years of operation, a thorough analysis of STRAW data has been performed and the results were highlighted in this presentation. The preliminary attenuation lengths measured with STRAW reach a peak of  $29.6^{+2.4}_{-1.8}$  m at 450 nm. Beyond just measuring the optical properties of the water, STRAW data was used to analyze the undersea light background which consists primarily of marine bioluminescence and Cherenkov emissions from radioactive decays. The former contributes to higher rate intense spikes, up to the STRAW DAQ saturation limit of 10 MHz whereas the latter contributes to a roughly 10 kHz constant baseline. Overall, the results from STRAW are promising and in good accordance with the site characteristics required for a neutrino telescope.

#### References

- [1] Agostini, M and et al., Nature Astronomy (2020).
- [2] M. Boehmer et al., Journal of Instrumentation **14**, P02013 (2019).
- [3] F. Henningsen et al., JINST **15**, P07031 (2020).
- [4] R. C. Smith and K. S. Baker, Applied Optics **20**, 177 (1981), Publisher: Optical Society of America.
- [5] D. Foreman-Mackey, D. W. Hogg, D. Lang, and J. Goodman, Publications of the Astronomical Society of the Pacific **125**, 306 (2013), arXiv: 1202.3665.

**Full Authors List: P-ONE Collaboration**

Nicolai Bailly<sup>1</sup>, Jeannette Bedard<sup>1</sup>, Michael Böhmer<sup>2</sup>, Jeff Bosma<sup>1</sup>, Dirk Brussow<sup>1</sup>, Jonathan Cheng<sup>1</sup>, Ken Clark<sup>3</sup>, Beckey Croteau<sup>1</sup>, Matthias Danninger<sup>4</sup>, Fabio De Leo<sup>1</sup>, Nathan Deis<sup>1</sup>, Matthew Ens<sup>4</sup>, Rowan Fox<sup>1</sup>, Christian Fruck<sup>2</sup>, Andreas Gärtner<sup>5</sup>, Roman Gernhäuser<sup>2</sup>, Darren Grant<sup>6</sup>, Helen He<sup>1</sup>, Felix Henningsen<sup>7</sup>, Kilian Holzapfel<sup>2</sup>, Ryan Hotte<sup>1</sup>, Reyna Jenkyns<sup>1</sup>, Hamish Johnson<sup>4</sup>, Akanksha Katil<sup>5</sup>, Claudio Kopper<sup>6</sup>, Carsten B. Krauss<sup>5</sup>, Ian Kulin<sup>1</sup>, Klaus Leismüller<sup>2</sup>, Sally Leys<sup>8</sup>, Tony Lin<sup>1</sup>, Paul Macoun<sup>1</sup>, Thomas McElroy<sup>5</sup>, Stephan Meighen-Berger<sup>2</sup>, Jan Michel<sup>9</sup>, Roger Moore<sup>5</sup>, Mike Morley<sup>1</sup>, Laszlo Papp<sup>2</sup>, Benoit Pirene<sup>1</sup>, Tom Qiu<sup>1</sup>, Mark Rankin<sup>1</sup>, Immacolata Carmen Rea<sup>2</sup>, Elisa Resconi<sup>2</sup>, Adrian Round<sup>1</sup>, Albert Ruskey<sup>1</sup>, Ryan Rutley<sup>1</sup>, Christian Spannfellner<sup>2</sup>, Jakub Stacho<sup>4</sup>, Ross Timmerman<sup>1</sup>, Meghan Tomlin<sup>1</sup>, Matt Tradewell<sup>1</sup>, Michael Traxler<sup>10</sup>, Matt Uganecz<sup>1</sup>, Seann Wagner<sup>1</sup>, Juan Pablo Yañez<sup>5</sup>, Yinsong Zheng<sup>1</sup>

<sup>1</sup>Ocean Networks Canada, University of Victoria, Victoria, British Columbia, Canada.

<sup>2</sup>Department of Physics, Technical University of Munich, Garching, Germany.

<sup>3</sup>Department of Physics, Engineering Physics and Astronomy, Queen's University, Kingston, Ontario, Canada.

<sup>4</sup>Department of Physics, Simon Fraser University, Burnaby, British Columbia, Canada.

<sup>5</sup>Department of Physics, University of Alberta, Edmonton, Alberta, Canada.

<sup>6</sup>Department of Physics and Astronomy, Michigan State University, East Lansing, MI, USA.

<sup>7</sup>Max-Planck-Institut für Physik, Munich, Germany.

<sup>8</sup>Department of Biological Sciences, University of Alberta, Edmonton, Alberta, Canada.

<sup>9</sup>Institut für Kernphysik, Goethe Universität, Frankfurt, Germany.

<sup>10</sup>Gesellschaft für Schwerionenforschung, Darmstadt, Germany.